First-principles study of high-pressure alumina polymorphs

Wenhui Duan, Renata M. Wentzcovitch, and Kendall T. Thomson
Department of Chemical Engineering and Materials Science, and Minnesota Supercomputer Institute, University of Minnesota, Minneapolis, Minnesota 55455
(Received 23 September 1997)

We investigate by first principles the structural properties and relative stability of six alumina polymorphs, namely: corundum, Rh_2O_3 (II), *Pbnm* perovskite, $R\bar{3}c$-perovskite, *A*-type rare-earth sesquioxide, and *B*-type rare-earth sesquioxide. The compressive behavior and pressure-induced changes in the local environment of different aluminum sites are investigated in detail for corundum, Rh_2O_3 (II) and the perovskite phases, which are the predicted stable phases within the pressure range of 0–450 GPa. This information is crucial for understanding the electronic states of a Cr^{+3} color center in alumina (ruby) and the resulting intra-*d* transitions, i.e., the ruby fluorescence. Implications of these pressure-induced phase transitions in Al_2O_3 to the ruby fluorescence pressure scale are discussed. [S0163-1829(98)09517-4]

I. INTRODUCTION

The structural and electronic properties of Al_2O_3, α-alumina, are of considerable importance due to the diverse applications of this material, particularly in high-pressure science. The pressure dependence of the *R* fluorescence lines of Cr^{+3}-doped Al_2O_3 corundum (ruby) provides the convenient and accurate technique of determining pressure in diamond-anvil-cell experiments.[1–6] The shift of *R* lines has been calibrated as a function of pressure (ruby scale) up to 180 GPa under nonhydrostatic conditions[2] and up to 110 GPa under quasihydrostatic conditions.[3] Extrapolation of the ruby scale has been used widely to determine pressures up to 460–550 GPa.[4] This range is far in excess of the calibrated maximum pressure, and thus this is an arguable procedure.[7] Although calibration of the pressure dependence of the luminescence spectrum does not require knowledge of the crystal structure or the microscopic environment of the Cr^{+3} ion, such knowledge is complementary, particularly when pressure is determined by extrapolations of the scale. Therefore, it is important to identify whether corundum transforms at high pressures and temperatures, since a phase change would most likely affect the nature and frequency of the fluorescence lines and bands.

Although previous room-temperature high-pressure experiments on alumina have shown an exceptional stability of corundum in a large pressure range,[4,8,9] many theoretical studies suggested that alternative phases might occur at elevated pressures.[10–14] Recently, a fully optimized first-principles calculation was conducted for four Al_2O_3 polymorphs, predicting corundum $\rightarrow Rh_2O_3(II) \rightarrow (Pbnm)$ orthorhombic-perovskite phase transformations.[14] The predicted transition pressure for corundum $\rightarrow Rh_2O_3$ (II) phase change (78 GPa) agrees reasonably well with that predicted by a linear augmented plane-wave calculation (90 GPa).[13] These theoretical predictions have recently been confirmed in a x-ray-diffraction experiment,[15] which observed that ruby undergoes a transformation to the Rh_2O_3 (II) structure when heated to 1000 K and pressurized to $\sim$100 GPa. Although the role of temperature in the experiment is not yet entirely clear, it appears that it allowed the transformation to occur by providing the required kinetics for this first-order transition.[14] Therefore, for future studies of ruby at ultrahigh pressure, it becomes important to understand how the structural transformations, in case they take place, would affect the ruby fluorescence lines.

In this paper, we make an attempt to identify such effects by investigating the behavior of the local environment of Al under pressure in different phases. The precise description of the structural deformation of alumina under pressure, will aid future theoretical and experimental studies of ruby under pressure, as well as the development of new interatomic potentials suitable for high-pressure studies as well.[16,17] We further investigate the relative stability of other candidate stable phases in this pressures range: the *A*- and *B*-type rare-earth sesquioxide structures (*A*- and *B*-RES).

In the next section, we describe the structures of the six investigated alumina polymorphs. In Sec. III, we present and discuss results on the relative stability of these polymorphs, the compressive behavior of the stable phases, and the change in the local environment of the aluminum sites under pressure in each of these structures. Our conclusions are summarized in Sec. IV.

II. ALUMINA STRUCTURES

Extensive reviews on high-pressure forms of A_2O_3-type compounds have been presented by Liu and Bassett,[18] and Reid and Ringwood.[19] Essentially, the systematics of phase transitions in these classes of compounds can be summarized as follows: (1) High-pressure polymorphs are denser than the zero-pressure forms, the coordination around the cation sites are higher, and packing is more efficient. (2) Sesquioxides of the A_2O_3 type may be divided into four groups:

(i) *The sesquioxides of the group V A elements.* These are loosely packed molecular compounds, and their structures should not be likely high-pressure forms.

(ii) *The sesquioxides of the group III A elements.* For these compounds the corundum structure is, in general, a high-pressure phase, and transitions from less dense β-Ga_2O_3 and *C*-type rare-earth sesquioxide (*C*-RES) struc-

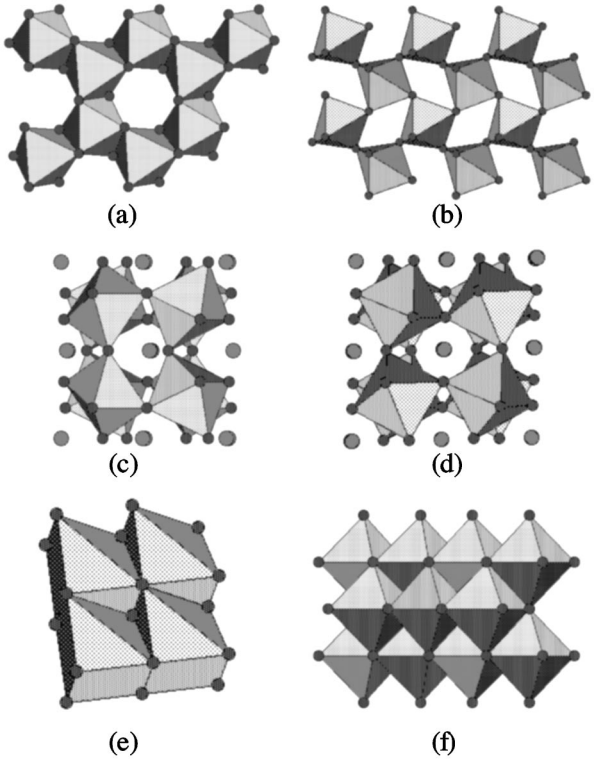

FIG. 1. (a) corundum, (b) Rh_2O_3 (II), (c) ($Pbnm$) orthorhombic-perovskite, (d) $R\bar{3}c$-perovskite, (e) A-RES, and (f) B-RES high-pressure phases of Al_2O_3. The oxygen atoms are represented as smaller spheres in all figures. Aluminum atoms are placed near the center of coordination polyhedra in all structures, as well as larger spheres in the perovskite structures (c) and (d).

tures to corundum have been reported in sesquioxides of Ga and In. Note that In_2O_3 transforms from corundum to a new phase at 11 GPa and 1100 °C.[20] This new phase was first suggested to be a perovskite-type structure (similar to orthorhombic perovskite $InRhO_3$),[20] and later suggested to be a Rh_2O_3 (II) structure.[18] Therefore, by analogy perovskite and Rh_2O_3 (II) forms are viable high-pressure candidates for Al_2O_3.

(iii) *The sesquioxides of the group III B and rare-earth elements.* The low-pressure phases of this group are C- and A-RES phases. At high pressure, the C-RES phase transforms to the B-RES phase. No pressure-induced phase transition was reported for the A-RES phase which is slightly denser than B-RES. Cations are, in general, sevenfold coordinated in the A-RES phase, and seven- and sixfold coordinated in the B-RES phase. Therefore, both A- and B-RES structures should be candidate high-pressure forms of Al_2O_3.

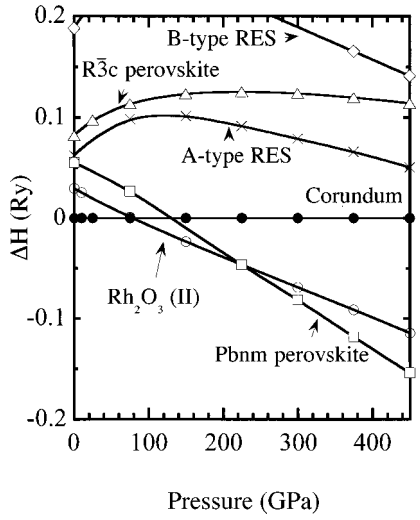

FIG. 2. Pressure dependence of the enthalpy relative to corundum for six Al_2O_3 phases: corundum (●), Rh_2O_3 (II) (○), ($Pbnm$) orthorhombic-perovskite (□), $R\bar{3}c$-perovskite (△), A-RES (×), and B-RES (◇).

(iv) *The sesquioxides of the trivalent transition elements.* Most of these compounds exist in the corundum phase at ambient conditions. Among them, Rh_2O_3 was found to transform from corundum to the Rh_2O_3 (II) phase at high pressures and temperatures.[21] This is the only experimentally confirmed pressure-induced transition from the corundum structure. Fe_2O_3 was observed to undergo a phase transition in the range of 40 to 80 GPa.[22] The high-pressure phase was tentatively assigned to be a perovskite form, or less possibly the B-RES structure.[22] Others have suggested that this transition would involve simply a change in the magnetic structure, similar to the high-spin to low-spin transition observed in Co_2O_3.[23]

Here, we investigate the relative stability of six possible Al_2O_3 high-pressure phases: corundum, Rh_2O_3 (II), ($Pbnm$) orthorhombic-perovskite, $R\bar{3}c$-perovskite, A- and B-RES. Their zero-pressure crystal structures are shown in Fig. 1. In all these phases, aluminum is coordinated by at least six oxygens. The corundum structure [Fig. 1(a)] has been experimentally observed up to 175 GPa.[9] Its space group is $R\bar{3}c$ with a rhombohedral unit cell containing 10 atoms (2 Al_2O_3). Rh_2O_3 (II) [Fig. 1(b)] is a theoretically predicted high-pressure phase of Al_2O_3,[13,14] and was observed in recent x-ray diffraction experiment.[15] It has space group $Pbna$ with an orthorhombic unit cell containing 20 atoms (4 Al_2O_3). The Rh_2O_3 (II) structure may be thought of as containing slabs of the corundum structure cut parallel

TABLE I. Summary of phase transition data for the predicted transformations in Al_2O_3: transition pressure P_T, transition volume V_T for one formula unit in the lower pressure phase, and fractional volume change $\Delta V/V_T$.

	Corundum — Rh_2O_3(II)			Rh_2O_3 (II) — Orthorhombic-perovskite
	This work	Ref. 11	Ref. 13	This work
P_T (GPa)	78±4	6∼62	91±6	223±15
V_T (Å^3)	34.60			28.70
$\Delta V/V_T$ (%)	−2.2	−2.3	−2.2	−2.2

TABLE II. Structural properties and cohesive energy for the Al_2O_3 phases at zero pressure. Corundum and $R\bar{3}c$ perovskite lattice parameters (a_R, α, and c/a) are based on a hexagonal unit cell. Internal positions for Al and O are reported for each structure in terms of their respective coordinate system. Experimental values for corundum are from Ref. 33 except for the cohesive energy which was calculated from Ref. 34.

	Corundum			Orthorhombic	$R\bar{3}c$ perovskite		
	Calc.	Expt.	Rh_2O_3 (II)	perovskite		A-type RES	B-type RES
Group	$R\bar{3}c$		$Pbcn$	$Pbnm$	$R\bar{3}c$	$C\bar{3}m$	$C2/m$
a_R (Å)	5.107	5.136			5.121		
α	55.41	55.286			56.77		
c/a (hex.)	2.72	2.73			2.64		
a (Å)			6.990	4.734		2.859	8.749
b (Å)			4.792	4.863		a	4.068
c (Å)			4.927	7.229		6.304	8.016
β							101.07
$Al^{(1)}$	(0.352,0.352,0.352)	(0.352,0.352,0.352)	(0.110,0.753,0.032)	(0.500,0.000,0.500)	(0.000,0.000,0.000)	(0.333,0.667,0.217)	(0.666,0.000,0.578)
$Al^{(2)}$				(0.510,0.549,0.250)	(0.250,0.250,0.250)		(0.664,0.000,0.141)
$Al^{(3)}$							(0.089,0.000,0.305)
$O^{(1)}$	(0.555,0.945,0.250)	(0.556,0.944,0.250)	(0.846,0.607,0.102)	(0.142,0.412,0.250)	(0.890,0.610,0.250)	(0.000,0.000,0.000)	(0.500,0.000,0.000)
$O^{(2)}$			(0.000,0.049,0.250)	(0.173,0.176,0.575)		(0.333,0.667,0.675)	(0.188,0.000,0.232)
$O^{(3)}$							(0.856,0.000,0.141)
$O^{(4)}$							(0.853,0.000,0.469)
$O^{(5)}$							(0.537,0.000,0.357)
E_c (eV)	7.34	6.33	7.26	7.19	7.12	7.17	6.83

to the $(10\bar{1}1)$ plane which is the most common twinning plane of corundum crystal.[21] In corundum and Rh_2O_3 (II), there is only one kind of aluminum site: edge-sharing AlO_6 octahedra. In the Rh_2O_3 (II) phase, octahedra share two edges with others, while in corundum they share three.

The orthorhombic ($Pbnm$) perovskite structure [Fig. 1(c)] is another possible high-pressure phase, and a previous calculation has shown that this must be the stable phase above 223 GPa.[14] This is the stable structure of $MgSiO_3$ perovskite, the major earth-forming mineral, presumably over the entire range of pressures prevailing in the earth's lower mantle. It has 20 atoms (4 Al_2O_3) in its orthorhombic unit cell. The $R\bar{3}c$-perovskite structure [Fig. 1(d)] is found in some rare-earth orthoaluminates $RAlO_3$ (Ref. 24) (R = La, Pr, or Nd) and could also be energetically favored in some pressure range. The A-RES structure [Fig. 1(e)] has metal atoms sevenfold coordinated, and is the stable form of the sesquioxides R_2O_3 (R= La, Ce, Pr, and Nd).[25] It has space group $C\bar{3}m$ with a hexagonal unit cell containing only one Al_2O_3 molecule. The RO_7 group is obtained from an octahedron by adding a seventh oxygen atom along a threefold axis. The B-RES structure [Fig. 1(f)] is monoclinic with space group $C2/m$ and contains 30 atoms (6 Al_2O_3) per unit cell.[26] There are three crystallographically distinct sites for metal atoms in this structure. Typically, two of them are sevenfold coordinated by oxygens, while the third site is sixfold coordinated, but has a somewhat longer bond to a seventh oxygen atom.

III. RESULTS AND DISCUSSION

Our results were obtained using a first-principles implementation of a variable cell shape molecular-dynamics algorithm,[27] which has been successfully applied to determine the compressive and elastic properties of important minerals under pressure.[14,28–30] We used the norm-conserving Troullier-Martins pseudopotentials[31] with partial core corrections[32] coupled with plane-wave energy cutoffs of 70 Ry for wave functions and 280 Ry for charge densities and potentials. Brillouin-zone summations were performed over two k points in the irreducible wedge ($2\times2\times2$ Monkhorst-Pack grid) for all structures except for A-RES, where the summation was performed over three k points. For the dynamical optimizations, fictitious cell mass and ionic masses were adjusted to produce similar oscillation periods for strains and ionic coordinates, and time steps were adjusted to produce approximately ten steps per period. Typically, 20–30 time steps are needed for full structural relaxations.

A. Phase stability and structural properties

Figure 2 shows the enthalpies of the six polymorphs relative to corundum. As previously shown,[14] Al_2O_3 is predicted to transform from corundum to the Rh_2O_3 (II) modification at 78 ± 4 GPa and then to the orthorhombic perovskite ($Pbnm$) structure at 223 ± 15 GPa. We find that, at zero pressure, all aluminum atoms in the B-RES phase are sixfold coordinated, but have two somewhat longer bonds to other oxygens. The longer bonds are more easily compressed, which leads to eightfold coordination at high pressures (225

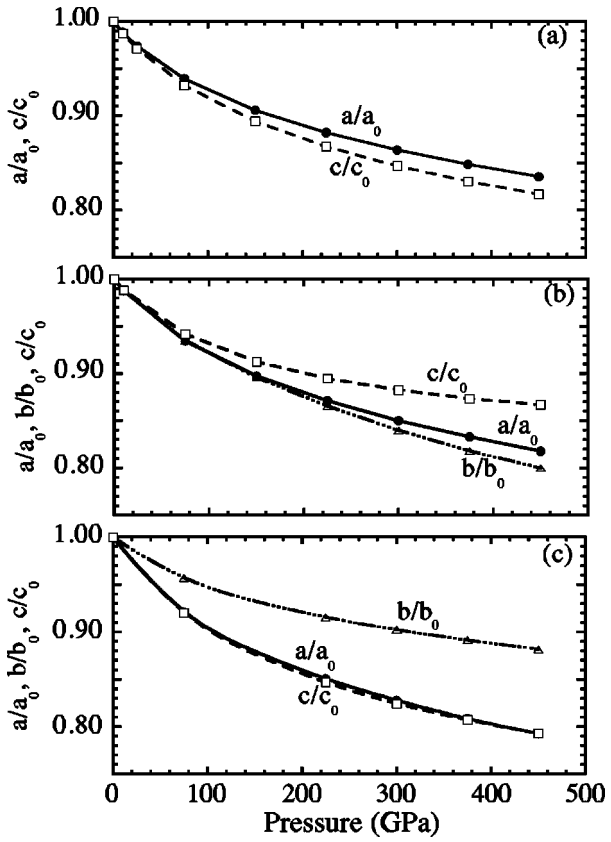

FIG. 3. Pressure dependence of the lattice parameters for the Al_2O_3 phases: (a) corundum, (b) Rh_2O_3 (II), (c) ($Pbnm$) orthorhombic-perovskite. a_0, b_0, and c_0 are zero-pressure values.

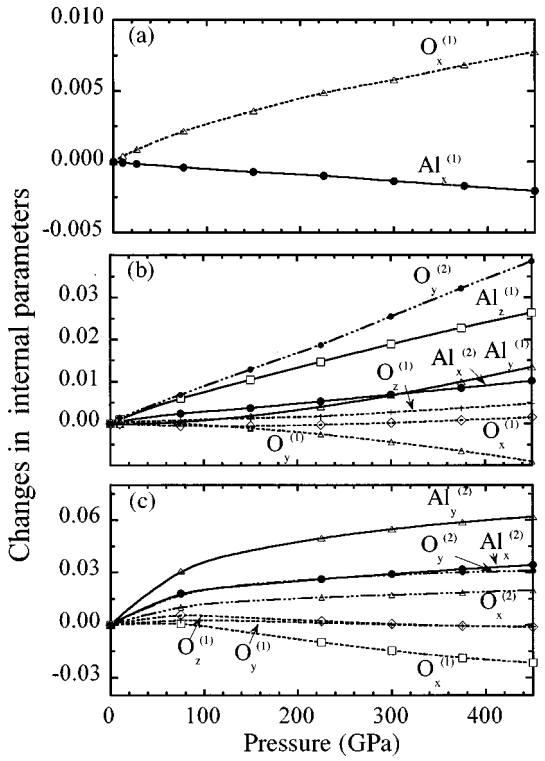

FIG. 4. Changes in internal parameters with pressure for Al_2O_3 phases: (a) corundum, (b) Rh_2O_3 (II), (c) ($Pbnm$) orthorhombic-perovskite.

GPa). This is quite different from the typical B-RES compounds in which metal atoms are sevenfold coordinated.

The A- and B-RES phases are found not to be competitive in the entire pressure range investigated, even though the aluminum polyhedra have larger coordination numbers. The reason for this, as well as for the atypical sevenfold coordination found in this phase, might lie in the fact that the sevenfold coordinated sites have lower symmetry and might provide an energetically stable environment (by splitting bonding and antibonding states) only for cations with partially filled electronic shells, as it occurs with rare-earth elements. The calculated phase transition data of the Al_2O_3 phases are summarized in Table I. Table II gives calculated structural parameters for all six Al_2O_3 phases at zero pressure. For corundum, all the calculated lattice parameters and internal positions of atoms are in excellent agreement with the data from x-ray experiments.[33,34]

The change in structural parameters versus pressure for the three stable phases is shown in Figs. 3 and 4. These numbers reveal that the compressive behavior of these phases differ. Their bulk moduli were calculated to be 259, 262, and 235 GPa for corundum, Rh_2O_3 (II), and $Pbnm$ perovskite, respectively.[14] Therefore, the perovskite framework must be somewhat more flexible in order to adapt better under pressure, since this is the densest phase as well. This picture is essentially confirmed in Fig. 4, where we see the largest changes in internal parameters under pressure for the perovskite phase. Although the corundum and Rh_2O_3 (II) phases have similar bulk moduli, Fig. 3 in particular shows that Rh_2O_3 (II) compresses considerably more anisotropically. The numbers reported in Figs. 3 and 4, and Table II, should be useful for future experimental and theoretical studies of pure and doped Al_2O_3 under pressure.

B. Compressive behavior of Al sites

Direct comparison of the structural parameters in different phases under pressure gives an overall idea of the degree of distortion experienced by the compressed frameworks. However, we are particularly concerned in anticipating the effect of phase transformations experienced by Al_2O_3 on the fluorescence lines of ruby, i.e., the ruby scale.[1–6] In ruby, Cr^{+3} enters as a substitutional impurity for aluminum. Several qualitative predictions regarding the nature of d-level splittings can already be made by combining crystal-field theory with information about the behavior of the local environment of different aluminum sites under pressure, i.e., point symmetry, bond lengths, and bond angles versus pressure.

Information about different aluminum sites in three stable structures [corundum, Rh_2O_3 (II) and ($Pbnm$) orthorhombic-perovskite] is summarized in Figs. 5 and 6. Internal bond lengths versus pressure for all polyhedra under consideration are shown in Figs. 5(a)–5(d). The average of the six shortest bond lengths for these phases is shown in Fig. 5(e). At zero pressure Cr^{+3} has larger ionic radius than Al^{+3} (0.615 Å compared to 0.535 Å),[35] therefore, we expect that it will prefer sites with larger average Al-O bond lengths, if within reasonable bounds, whenever there is a choice. The corundum and Rh_2O_3 (II) phases have only one kind of crystallographic site each, with point symmetries $C3$ and $C1$, respectively. The first noticeable feature throughout

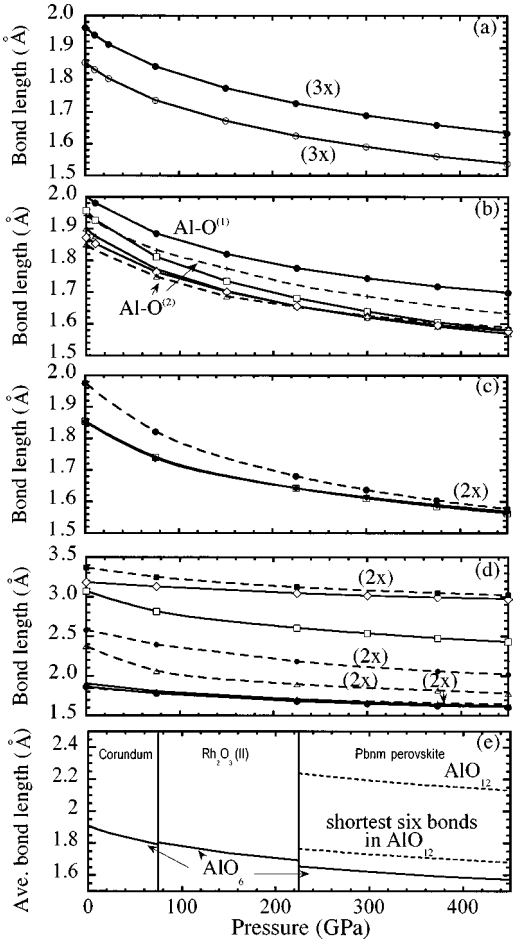

FIG. 5. Pressure dependence of the internal bond lengths of the AlO_6 octahedra in the Al_2O_3 phases: (a) corundum, (b) Rh_2O_3 (II), and (c) ($Pbnm$) orthorhombic-perovskite. The internal bond lengths of the AlO_{12} polyhedron in the ($Pbnm$) orthorhombic-perovskite phase are also given in (d) for comparison. There are two crystallographically distinct oxygen sites in Rh_2O_3 (II) and ($Pbnm$) perovskite, and the Al-O bondlengths at these sites are plotted in solid and dashed lines. (e) The average Al-O bond lengths for the stable phases throughout their predicted stability fields. For the perovskite phase, we also plot the average of the smallest six bondlengths of the AlO_{12} polyhedron.

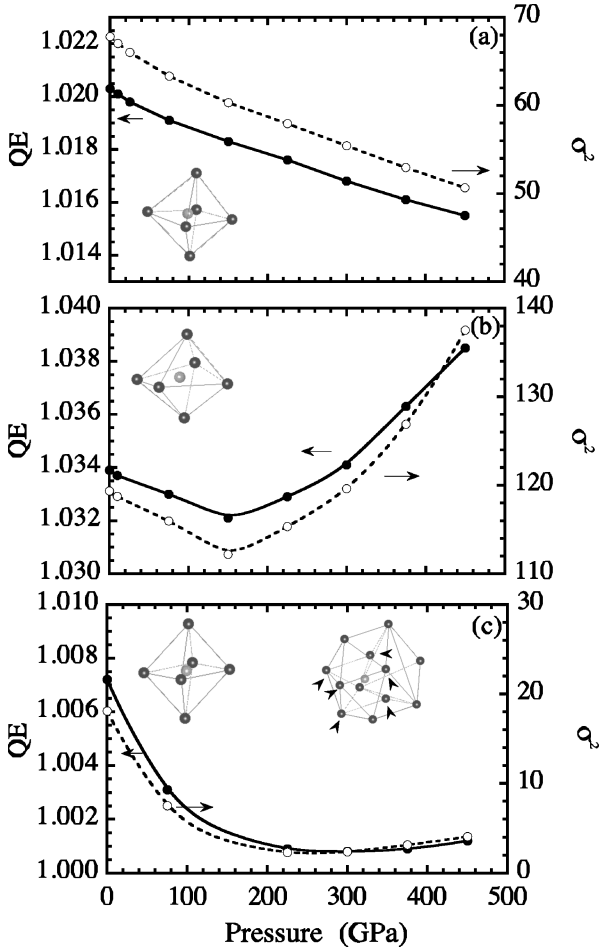

FIG. 6. Pressure dependence of quadratic elongations QE (——) and angle variances σ^2 (– – –) (as defined by Ref. 36) of the AlO_6 octahedra for the Al_2O_3 phases: (a) corundum, (b) Rh_2O_3 (II), and (c) $Pbnm$-perovskite. Insets show octahedral shapes. In (c) the coordination shell of the 12-fold site in $Pbnm$-perovskite is also shown. The nearest six neighbors are indicated by arrows.

the corundum to Rh_2O_3 (II) transformation at 78 GPa is the symmetry lowering and the splitting of bond lengths, which implies further d-level splittings. This suggests that if this transformation were to occur, the ruby fluorescence lines and bands might broaden. Only an accurate calculation of the impurity states would allow us to assess the nature of the frequency shifts, but the similarity among average bondlengths across the transformation [Fig. 5(e)] suggests that such shifts might be a minor effect.

In the perovskite phase, there are two possible distinct sites for Cr^{+3}: an octahedral one ($Al^{(1)}$ in Table II) with symmetry C_i, and a formally 12-fold site ($Al^{(2)}$ in Table II) with symmetry C_{1h}. The internal and average bondlengths for these two sites are shown in Figs. 5(c)–5(e). The internal bond lengths around the 12-fold site span a wide range of distances, however only the six shortest bonds are within the pressure range spanned by the Al-O bond lengths in the other structures. Presumably, the strongest Al-O bonds involve only the first six oxygen neighbors, and the average value of these bonds is also shown in Fig. 5(e). Throughout the Rh_2O_3 (II) to perovskite transformation, the average bondlength around the $Al^{(1)}$ site decreases, while that around the $Al^{(2)}$ site increases considerably, or only mildly if we consider the six shortest Al-O bonds. With a good degree of confidence, it can be said that Cr^{+3} will prefer the $Al^{(2)}$ site since the average bondlength in this site corresponds more closely to the Cr-O bondlength. This suggests that d-level splittings will be smaller than in the Rh_2O_3 (II) phase, and intra-d level transitions will be red-shifted. This scenario derives from simple considerations based on the one electron picture. Considerations of the fully correlated multiplet states might render these trends less significant.

Finally, we quantify, by means of quadratic elongations (QE) and angle variances (σ^2),[36] the degree of distortion of the sixfold sites in the three structures considered. They are defined as[36]

$$\sigma^2 = \sum_{i=1}^{12} (\theta_i - 90°)^2/11$$

and

$$\mathrm{QE}=\sum_{i=1}^{6}(l_i/l_0)^2/6,$$

where θ_i's are the octahedral internal angles and l_i's are the center-to-vertex distances of the distorted octahedron. l_0 is the center-to-vertex distance of a regular octahedron having the same volume as that of the distorted octahedron. For regular polyhedra, QE and σ^2 are 1 and 0, respectively. Departure from these values indicates the degree of distortion away from perfect O_h symmetry. Figure 6(a) shows that in corundum, octahedral distortions decrease with increasing pressure. Therefore, the assumption of nearly O_h and constant symmetry for this site, as made in some previous theoretical studies of the Cr^{+3} impurity of ruby, describes closely the real physical situation. In contrast, Fig. 6(b) shows that in the Rh_2O_3 (II) phase octahedra are considerably more distorted, and the distortion increases further beyond 150 GPa. This will have the effect of further splitting the e and t_{2g} levels in Cr^{+3}. Figure 6(c) shows that the purely octahedral $Al^{(1)}$ site in the perovskite phase is the least distorted one. On the other hand, the first six neighbors to the $Al^{(2)}$ site depart considerably from octahedron symmetry, resembling more closely to a triangular slab. This should be the preferred site for the Cr^{+3} impurity.

IV. SUMMARY

In summary, we have investigated the relative stability of six Al_2O_3 alumina polymorphs in the range of 0–450 GPa. For the three predicted stable phases in this pressure range, i.e., corundum, Rh_2O_3 (II), and *Pbnm*-perovskite, we present the pressure dependence of all structural parameters that characterize these phases. We also describe in detail the change of local environment of all aluminum sites in these stable phases. We show that across the corundum to Rh_2O_3 phase transformation, the octahedral site distorts significantly. In the last phase, there are two considerably different sites, and a Cr^{+3} impurity should prefer the 12-fold site (in fact, a highly distorted sixfold site). This information should be useful for experimental studies searching for high-pressure phases as well as for theoretical studies of Cr^{+3}-doped alumina, i.e., the effect of phase transformations on the ruby-fluorescence lines.

ACKNOWLEDGMENTS

This research was supported by the Minnesota Supercomputer Center, the Center for Interfacial Engineering (an NSF Engineering Research Center), and the National Science Foundation through Grant No. EAR-9628199 to R.M.W.

[1] R. A. Forman, G. J. Piermarini, J. D. Barnett, and S. Block, Science **176**, 284 (1972).

[2] P. M. Bell, H.-K. Mao, and K. Goettel, Science **226**, 542 (1984); P. M. Bell, J.-A. Xu, and H. K. Mao, in *Shock Waves in Condensed Matter*, edited by Y. M. Gupta (Plenum, New York, 1986), p. 125.

[3] H.-K. Mao, J.-A. Xu, and P. M. Bell, J. Geophys. Res. **91**, 4637 (1986); R. J. Hemley, C. S. Zha, A. P. Jephcoat, H. K. Mao, and L. W. Finger, and D. E. Cox, Phys. Rev. B **39**, 11 820 (1989).

[4] J.-A. Xu, H.-K. Mao, and P. M. Bell, Science **232**, 1404 (1986).

[5] Y. M. Gupta and X. A. Shen, Appl. Phys. Lett. **58**, 583 (1991); S. M. Sharma and Y. M. Gupta, Phys. Rev. B **43**, 879 (1991); Y. M. Gupta, P. D. Horn, and J. A. Burt, J. Appl. Phys. **76**, 1784 (1994).

[6] J. H. Eggert, K. A. Gottel, and I. F. Silvera, Phys. Rev. B **40**, 5724 (1988); **40**, 5733 (1988); J. H. Eggert, F. Moshary, W. J. Evans, K. A. Gottel, and I. F. Silvera, *ibid.* **44**, 7202 (1991).

[7] Y. K. Vohra, C. A. Vanderborgh, S. Desgreniers, and A. L. Ruoff, Phys. Rev. B **42**, 9189 (1990); J. H. Eggert, K. A. Goettel, and I. F. Silvera, *ibid.* **42**, 9191 (1990).

[8] P. Richet, J.-A. Xu, and H.-K. Mao, Phys. Chem. Miner. **16**, 207 (1988).

[9] A. P. Jephcoat, R. J. Hemley, H. K. Mao, and K. A. Goettel, Physica B **150**, 116 (1988).

[10] R. E. Cohen, Geophys. Res. Lett. **14**, 37 (1987).

[11] H. Cynn, D. G. Isaak, R. E. Cohen, M. F. Nicol, and O. L. Anderson, Am. Mineral. **75**, 439 (1990).

[12] M. S. T. Bukowinski, A. Chizmeshya, G. H. Wolf, and H. Zhanh, Mol. Eng. **6**, 81 (1996).

[13] F. C. Marton and R. E. Cohen, Am. Mineral. **79**, 789 (1994).

[14] K. T. Thomson, R. M. Wentzcovitch, and M. S. T. Bukowinski, Science **274**, 1880 (1996).

[15] N. Funamori and R. Jeanloz, Science **278**, 1109 (1997).

[16] M. Wilson, M. Exner, Y. Huang, and M. W. Finnis, Phys. Rev. B **54**, 15 683 (1996).

[17] P. Kizler, J. He, D. R. Clarke, and P. R. Kenway, J. Am. Ceram. Soc. **79**, 3 (1996).

[18] L. Liu and W. A. Basset, *Elements, Oxides, Silicates: High-Pressure Phases with Implications for the Earth's Interior* (Oxford University Press, Oxford, 1986).

[19] A. F. Reid and A. E. Ringwood, J. Geophys. Res. **74**, 3238 (1969).

[20] M. Marezio, A. Waintal, J. Chenavas, J. J. Capponi, and M. Gondrand, in *Les Propiétés Physiques des Solids Sous Pression*, edited by R. Georges and R. Maury (Centre National de la Recherche Scientifique, Paris, 1970), p. 403.

[21] R. D. Shannon and C. T. Prewitt, J. Solid State Chem. **2**, 134 (1970).

[22] T. Goto, J. Sato, and Y. Syono, in *High-Pressure Research in Geophysics*, edited by S. Akimoto and M. H. Manghnani (CAPJ, Tokyo, 1982), p. 595.

[23] J. Chenavas and J. C. Joubert, Solid State Commun. **9**, 1057 (1971).

[24] R. D. Burbank, J. Appl. Crystallogr. **3**, 112 (1970); M. Marezio, P. D. Demier, and J. P. Remeika, J. Solid State Chem. **4**, 11 (1972).

[25] W. C. Koehler and E. O. Wollan, Acta Crystallogr. **6**, 741 (1953).

[26] D. T. Cromer, J. Phys. Chem. **61**, 753 (1956).

[27] R. M. Wentzcovitch, in *Quantum Theory of Real Materials*, edited by J. R. Chelikowsky and S. G. Louie (Kluwer Academic, Dordrecht, 1996), p. 113.

[28] R. M. Wentzcovitch, J. L. Martins, and G. D. Price, Phys. Rev. Lett. **70**, 3947 (1993).
[29] K. T. Thomson, R. M. Wentzcovitch, A. V. McCormick, and H. T. Davis, Chem. Phys. Lett. (to be published, 1998).
[30] C. Da Silva, L. Stixrude, and R. M. Wentzcovitch, Geophys. Res. Lett. **24**, 1963 (1997); B. Kiefer, L. Stixrude, and R. M. Wentzcovitch, *ibid.* **24**, 2841 (1997).
[31] N. Troullier and J. L. Martins, Phys. Rev. B **43**, 1993 (1991).
[32] S. G. Louie, S. Froyen, and M. L. Cohen, Phys. Rev. B **26**, 1738 (1982).
[33] H. d'Amour, D. Schiferl, W. Denner, H. Schulz, and W. B. Holzapfel, J. Appl. Phys. **49**, 4411 (1978).
[34] *CRC Handbook of Chemistry and Physics*, 66th ed., edited by R. C. Weast (CRC, Boca Raton, FL, 1985).
[35] R. G. Burns, *Mineralogical Applications of Crystal Field Theory*, 2nd ed. (Cambridge University Press, Cambridge, 1993).
[36] K. Robinson, G. V. Gibbs, and P. H. Ribbe, Science **172**, 567 (1971).